TU Delft

Delft University of Technology

A Variable Stability In-Flight Simulation System using Incremental Non-Linear Dynamic Inversion

Scholten, Pepijn; van Paassen, Rene; Mulder, Max

DOI
10.2514/6.2020-0852

Publication date
2020

Document Version
Final published version

Published in
AIAA Scitech 2020 Forum

Citation (APA)
Scholten, P., van Paassen, R., & Mulder, M. (2020). A Variable Stability In-Flight Simulation System using Incremental Non-Linear Dynamic Inversion. In *AIAA Scitech 2020 Forum: 6-10 January 2020, Orlando, FL* Article AIAA 2020-0852 (AIAA Scitech 2020 Forum; Vol. 1 PartF). American Institute of Aeronautics and Astronautics Inc. (AIAA). https://doi.org/10.2514/6.2020-0852

Important note
To cite this publication, please use the final published version (if applicable).
Please check the document version above.

Copyright
Other than for strictly personal use, it is not permitted to download, forward or distribute the text or part of it, without the consent of the author(s) and/or copyright holder(s), unless the work is under an open content license such as Creative Commons.

Takedown policy
Please contact us and provide details if you believe this document breaches copyrights.
We will remove access to the work immediately and investigate your claim.

This work is downloaded from Delft University of Technology.
For technical reasons the number of authors shown on this cover page is limited to a maximum of 10.

AIAA SciTech Forum
6-10 January 2020, Orlando, FL
AIAA Scitech 2020 Forum

10.2514/6.2020-0852

Check for updates

A Variable Stability In-Flight Simulation System using Incremental Non-Linear Dynamic Inversion

P.A.Scholten*, M.M. van Paassen†, Q.P. Chu‡and M. Mulder⊥
Delft University of Technology, 2629 Delft, The Netherlands

A variable stability in-flight simulator has the capabilities to change the response of an aircraft in-flight, often without changing the physical properties of the aircraft. The ability to adjust the aircraft response characteristics and handling qualities has various purposes, such as pilot training, control logic development and handling quality research. A variable stability control system is designed for a medium range business jet using Incremental Non-linear Dynamic Inversion. The performance of the in-flight simulator is verified by two experiments, one conducted in a fixed-base flight simulator and one in a Cessna Citation II laboratory aircraft. The fly-by-wire actuation system in the Cessna Citation II is based on its existing autopilot, inheriting the limited performance and safety protections.The simulator experiment shows differences between the experienced handling qualities for a reference model and the designed controller combined with aircraft dynamics. These differences mainly arise due to actuator saturation for specific handling quality settings. The in-flight experiment supports the simulator findings but also reveals how the available control authority around the initial condition is limited due to constraints of the fly-by-wire system.

Downloaded by TU DELFT on January 6, 2020 | http://arc.aiaa.org | DOI: 10.2514/6.2020-0852

Nomenclature

α	=	Angle of attack [*rad*]
β	=	Sideslip angle [*rad*]
δ_a, δ_e	=	Aileron, elevator deflection [*rad*]
$\dot{\phi}, \dot{\theta}$	=	Roll, pitch rate [*rad/s*]
ω	=	Angular acceleration [rad/s^2]
ω_c	=	Crossover frequency [*rad/s*]
ω_p, ω_q	=	Roll, pitch natural frequency [*rad/s*]
ω_{sp}	=	Aircraft short period natural frequency [*rad/s*]
$\overline{c}$	=	Mean aerodynamic chord [m]
ϕ, θ	=	Roll, pitch angle [*rad*]
ρ	=	Air density [kg/m^3]
ζ_p, ζ_q	=	Roll, pitch damping ratio
ζ_{sp}	=	Aircraft short period damping ratio
b	=	Wing span [m]
C_*	=	Aircraft dynamic coefficients
J	=	Inertia tensor
K_*	=	Control gains
M_a	=	Moment induced by the airframe [Nm]
M_c	=	Moment induced by the control effectors [Nm]
M_T	=	Moment induced by thrust [Nm]
$n_{z_{ss}}$	=	Normal steady state acceleration [*m/s*]
p, q, r	=	Roll, pitch and yaw rate [*rad/s*]
S	=	Wing surface area [m^2]
T_{θ_2}	=	Longitudinal pitch response coefficient [s]
u, u_p	=	Input and pilot input
u_{mod}	=	Modified input after reference model
u_{req}	=	Requested input after sidestick gains [*rad*]
V	=	Airspeed [*m/s*]
v_h	=	Hedging signal
V_{ias}	=	Indicated airspeed [*m/s*]
V_{tas}	=	True airspeed [*m/s*]
x	=	Aircraft states
CAP	=	Control Anticipation Parameter
DUECA	=	Delft University Environment for Communication and Activation
FAST	=	Full-scale Advanced System Testbed
FL	=	Flight Level
HMI Lab	=	Human Machine Interaction Laboratory
HOS	=	High Order System
IMU	=	Inertial Measurement Unit
INDI	=	Incremental Non-linear Dynamic Inversion
LOES	=	Low Order Equivalent System
NASA	=	National Aeronautics and Space Administration
NLR	=	Netherlands Aerospace Centre
PCH	=	Pseudo-Control Hedging
PID	=	Proportional Integral Derivative
PIO	=	Pilot Induced Oscillations
VISTA	=	Variable In-flight Simulator Test Aircraft

*Researcher, Control and Simulation, Faculty of Aerospace Engineering, Kluyverweg 1; p.a.scholten@live.nl
†Associate Professor, Control and Simulation, Faculty of Aerospace Engineering, Kluyverweg 1; m.m.vanpaassen@tudeft.nl. Member AIAA
‡Associate Professor, Control and Simulation, Faculty of Aerospace Engineering, Kluyverweg 1; q.p.chu@tudeft.nl. Member AIAA
⊥Professor, Control and Simulation, Faculty of Aerospace Engineering, Kluyverweg 1; m.mulder@tudelft.nl. Associate Fellow AIAA

I. Introduction

Training of test pilots requires them to experience a variation of handling qualities. It would require different aircraft to provide these handling qualities, significantly increasing training costs. A variable stability in-flight simulator is a system which has the capabilities to change the response of an aircraft *in-flight*, often without changing the physical properties of the aircraft. It allows adjustments of response characteristics and handling qualities. An aircraft equipped with such a system

Copyright © 2020 by Delft University of Technology. Published by the American Institute of Aeronautics and Astronautics, Inc., with permission.

can mimic the response of other aircraft, also during flight. Apart from training benefits, such a system can also be used for control law development and handling quality research [1].

In the early years, variable stability simulators were used to design control logic for different flight situations, like landing on an aircraft carrier [2]. In the 1970s and 1980s, focus moved from specific flight situations or aircraft configurations to testing conceptual control logic of novel aircraft. More recent developments show the possibility for the in-flight simulator to follow the dynamics of different aircraft [2].

Different methods have been investigated to modify the handling qualities using variable stability. The response feedback method, is a basic method that feeds back the aircraft response to modify the control inputs, Mirza et al. [3]. This enables one to modify the handling qualities, but does not offer direct selection. A more advanced method, which enables selection of handling qualities, is model-following [4]. It forces an aircraft to perform like a predetermined model [5] [6]. A drawback of both methods is that multiple linear controllers are required, and since an aircraft is a non-linear system, these controllers have to be gain-scheduled in the operating regime of the aircraft, requiring considerable tuning effort.

The non-linearities can also be accounted for by using dynamic inversion, a method that uses the differentiation of the aircraft output until the control input appears in the derivative [7]. Ko et al. [8] developed a variable stability system based on this principle, where the pitch, roll, yaw and normal load could be matched [9]. However, their research was limited to offline simulations and linearised aircraft models. Miller [10] introduced non-linear aircraft models and flew the variable stability system in a modified F-18. His implementation required full non-linear aircraft models and is thus constrained by the availability and accuracy of these models.

Incremental non-linear dynamic inversion (INDI) is a novel development in the field of dynamic inversion. It uses the aircraft accelerations and converts them to equivalent pitch, roll or yaw inputs using a moment effectiveness parameter [11]. A full non-linear aircraft model is not required anymore. Germann [12] designed a variable stability system using INDI for the T-6A Texan II aircraft. He linearised the moment effectiveness parameter which limited the performance of his system and he only tested the system in offline simulation. Grondman et al. [13] developed an INDI controller for the Cessna Citation II laboratory aircraft. Their controller was flown successfully but was not designed for variable stability.

These developments indicate the potential of INDI to achieve a variable stability system. It is beneficial over other techniques since it requires less gain scheduling, it does not require a full non-linear model of the aircraft dynamics and it enables the selection of handling qualities. The design and implementation of a variable stability system using INDI has not been attempted in previous research.

The purpose of this paper is twofold. First, it is investigated whether INDI can be used to create a variable stability in-flight simulator. This will be tested in offline simulation, a simulator experiment and in the Cessna Citation II laboratory aircraft operated by TU Delft and NLR. Second, the limits of such a system will be investigated. The fly-by-wire actuation system in the Cessna Citation II is based on its existing autopilot, inheriting the limited performance and safety protections[14, 15]. The control authority of the autopilot is restricted due to limitations in torque which are imposed on the actuator servo motors. Hence, the proposed system is expected to be limited by accuracy of the moment effectiveness and performance of the actuation system, and determining how these system limitations propagate to the INDI-based variable stability system is one of the main purposes of this research.

The paper is structured as follows. First some additional background information is presented in Section II. Second, the controller design is explained in Section III. The controller is tested in offline simulations in Section IV, in a flight simulator experiment in Section V and validated in real flight tests in Section VI. The paper ends with a Discussion and Conclusions.

II. Background

A. Variable Stability

1. Response feedback

Response feedback is the most basic method to achieve a variable stability system. The response output of the aircraft is measured and fed back to modify the control inputs. A mathematical description of this system is given by Nelson [16] and the solution technique for achieving a target response, using the Ricatti equations, is presented by Bryson and Ho [17]. Mirza et al. [3] found that response feedback is effective in changing the stability and handling qualities. Handling qualities that are changed by response feedback could be identified by the pilots in their experiment, even in a fixed-base simulation.

2. Model-following

A second method to achieve a variable stability system is model-following. The aircraft response is changed so it performs like a predetermined model. This is beneficial when designing aircraft to meet the specifications determined by regulations. Two different strategies, implicit or explicit model-following, are used to design model-following control systems, as originally described by Armstrong [4], O'Brien and Broussard [5] and Kreindler and Rothschild [6]. The implicit model-following technique is a basic method where gains are selected to reach the desired behaviour. In explicit model-following, the model to be followed is placed inside the control logic as a feedforward compensator.

3. Dynamic inversion

The previously presented control methods share the same drawback. Since an aircraft is a non-linear system, the described design tools require multiple linear controllers, which have to be gain-scheduled in the operating regime of the aircraft. Alternatively, these non-linearities can be accounted for with a technique called *dynamic inversion*. Slotine and Li [7]

Downloaded by TU DELFT on January 6, 2020 | http://arc.aiaa.org | DOI: 10.2514/6.2020-0852

developed the initial concept, which uses differentiation of the output until the control input appears in the derivative.

Such a linear dynamic inversion was implemented by Ko et al. [8] in a variable stability system. They used a model of the Korean next-generation fighter and used linear dynamic inversion to follow the dynamics of the F-16 fighter aircraft in offline simulations. Ko and Park [18] introduced an updated version of their system, which included a switching mechanism between the normal flight computer and the dynamic inversion model. Finally Ko and Park [9] introduced the normal load to their initial variable stability control system, that only could follow pitch, roll and yaw. However, they do not discuss the main limitation of linear dynamic inversion. The performance of the linear dynamic inversion is constrained by the performance of the linear model of the aircraft. This linear model, in turn, depends on both the accuracy of the model and the operating point where it is linearised.

Non-linear dynamic inversion solves some of these issues. It uses a model of the aircraft non-linear dynamics, in contrast to the previously used linear approximation. In practice, this means that full look-up tables have to be implemented in the controller. Miller [10] shows such an implementation for the FAST system from NASA, with hardware in the loop simulation experiments. However, recent developments within dynamic inversion provide a means to avoid the requirement of a full non-linear model of the aircraft.

4. Incremental non-linear dynamic inversion

Incremental non-linear dynamic inversion (INDI) uses the advantages from the dynamic inversion, but does not require the full non-linear aircraft model. The development of INDI can be traced back to Smith [11]. He acknowledges the issues with the non-linear dynamic inversion and proposes a new method using acceleration sensors. The accelerations are converted to an equivalent pitch, roll or yaw input using a moment effectiveness parameter (based on the moment due to control surface deflection and the aircraft inertia). He demonstrated that the INDI method provides considerable robustness regarding authority limits, sensor noise and significant variations within the control law (mainly inertia and control powers).

The combination of the actuator position sensor and the acceleration sensors ensure that angular accelerations are matched robustly. Germann [12] developed a variable stability system for the T-6A Texan II for the American Airforce based on INDI. He showed in offline simulations that the Texan II matches the dynamics of the F-16 aircraft. Bacon and Ostroff [19] used the INDI method to design a re-configurable flight control system in case of system failure. They acquired the angular accelerations by combining linear accelerations and differentiating the angular rates. This created noise and was considered to be sufficient but not optimal since the differentiation also introduced some time delays. Cox and Cotting [20] continued the development of the ideas from Smith, Bacon and Ostroff. They implemented the INDI logic in the ground-based simulators at NASA Dryden. The main takeaway from their work is that INDI is viable for real-time aircraft control and simulation, not just in an offline simulation.

Smeur et al. [21] [22] showed that the INDI controller performs better regarding gust resistance, compared to a normal Proportional Integral Derivative (PID) controller. Grondman et al. [13] developed an INDI controller for the Cessna Citation II, which was based on angular rate control. Their controller was flown successfully in the Cessna Citation II, but their controller was not designed for variable stability.

B. Handling Qualities

Handling qualities are defined as *"those qualities or characteristics of an aircraft that govern the ease and precision with which a pilot is able to perform the tasks required in support of an aircraft role"* [23]. This definition shows a clear combination of performance of the pilot and the aircraft acting together as a system for specific manoeuvres of the aircraft.

1. Control Anticipation Parameter

The Control Anticipation Parameter (CAP) is a longitudinal handling quality criterion which focuses on the short period pitch aircraft response. It was originally introduced by Bihrle [24], after which it became one of the criteria to measure longitudinal handling qualities, defined in the MIL-STD-1797A, Flying Qualities of Piloted Aircraft [25]. It is expressed as the ratio of initial pitch acceleration (second derivative of θ) to the normal acceleration in steady state $n_{z_{ss}}$:

$$CAP = \frac{\ddot{\theta}(0)}{n_{z_{ss}}} \tag{1}$$

Bischoff [26] argued that the CAP can be calculated from the short period characteristics of the aircraft. This method only holds for aircraft with a general second order longitudinal response as given in Equation 2. Based on this assumption, Bischoff rewrites Equation 1 to Equation 3:

$$\frac{q}{\delta_e} = \frac{K_\theta(s + \frac{1}{T_{\theta_2}})}{s^2 + 2\zeta_{sp}\omega_{sp}s + \omega_{sp}^2} \tag{2}$$

$$CAP \approx \frac{\omega_{n_{sp}}^2}{n/\alpha} \approx \frac{\omega_{n_{sp}}^2}{\frac{V}{g}\frac{1}{T_{\theta_2}}} \tag{3}$$

When the CAP is used as a handling quality criterion, it is always indicated in combination with the short period damping ratio. This criterion is categorised into different flight phases (A, B, C) and aircraft classes (I, II, III, IV). Within these categories, another segmentation exists into three different levels of acceptability (Level 1, 2 and 3).

- Level 1: Flying qualities are adequate for mission flight,
- Level 2: Flying qualities are adequate to accomplish the mission with increased pilot workload, and
- Level 3: Flying qualities cause inadequate mission effectiveness due to excessive pilot workload.

2. Low Order Equivalent System

The combined actuator and aircraft dynamics are of higher order compared to the second order longitudinal response as assumed by Bischoff. Di Franco [27] was one of the first to

Downloaded by TU DELFT on January 6, 2020 | http://arc.aiaa.org | DOI: 10.2514/6.2020-0852

research the effects of Higher Order System (HOS) dynamics on the longitudinal handling qualities. He determined that the aircraft short period response could be represented by a second-order equivalent term and a time delay. This was further developed into the Low Order Equivalent System (LOES) concept by Hodgkinson et al. [28]. They created an equivalent low order system by matching the complex frequency response of the higher order systems. In this way, a HOS can be represented as a low order system with a time delay term, and analytical methods developed for low order systems can be applied.

There are several techniques available to determine the LOES and their advantages and disadvantages are discussed by Mirza et al. [3]. The most robust method is the *Output Error* and *Equation Error* approach developed by Morelli [29]. The LOES method uses the equation error and output error parameter estimation in the frequency domain. They are two separate parameter estimation methods. The equation error method can estimate the parameters by fixing the time delay to a specific initial condition, whereas the output error method requires initial estimates for all parameters. However, the equation error method does not guarantee a global minimum. That is why Morelli suggested using the parameters from an initial equation error estimation as a guess for the output error estimation. This results in the estimation with the lowest error.

3. Cooper-Harper Rating

The Cooper-Harper rating scale is one of the accepted standards for subjective handling quality measurement. Cooper and Harper [23] developed a decision tree rating scale as a tool to assess aircraft handling quality. The scale takes qualitative pilot comments and translates them into a quantitative scale from 1 to 10. It can be used in experiments to find the handling qualities as experienced by the pilots.

III. Controller Design

A. Requirements

Before the initial design of the controller can be created, some requirements for this controller are determined. First, the implementation of the controller should be flexible, since the variable stability platform should be used for multiple in-flight simulation purposes. This implies that it can be used for multiple goals without having to change the basic logic. To enable this, an **inner loop** and **outer loop** have been defined, where the functionality of the inner loop is independent of the outer loop. The outer loop can be used to define the different control goals.

Secondly, the controller should take into account the limitations of the system dynamics, being the actuators and aircraft dynamics, respectively. This is most important for the experiment in the simulator since this experiment should give an indication of the theoretical performance of the in-flight simulator. The fly-by-wire system will impose limitations on the in-flight simulation capabilities, combined with the physical limitations of the aircraft dynamics.

Both requirements lead to the schematic block diagram of the controller structure, which is shown in Figure 1.

B. Inner Loop

1. INDI

The main benefit of the INDI method is that the INDI controller uses information from the system dynamics to adapt the moment effectiveness dependent on the flight condition. This way, parts of the aerodynamic moment M_A can be neglected in the model. The aerodynamic moment can be split into three main components, being the moment induced by thrust M_T, the moment induced by the control effectors M_c and the airframe dependent moment M_a.

It is assumed that the moment induced by the thrust can be neglected, $M_T \approx 0$. The airframe dependent moment and the moment induced by the control effectors are described by Equation 4 and Equation 5, respectively. In these equations, V_{tas} is the true airspeed, ρ is the air density, b is the wing span, $\overline{c}$ is the mean aerodynamic chord, S is the wing surface area and C_* are the aircraft's dynamic coefficients. These dynamic coefficients are defined by the system dynamics and retrieved from the aircraft model.

$$\boldsymbol{M_a} = \frac{1}{2}\rho V_{tas}^2 S \begin{bmatrix} bC_{l_a} \\ \overline{c}C_{m_a} \\ bC_{n_a} \end{bmatrix} \tag{4}$$

$$\boldsymbol{M_c} = \frac{1}{2}\rho V_{tas}^2 S \begin{bmatrix} bC_{l_{\delta_a}} & 0 & bC_{l_{\delta_r}} \\ 0 & \overline{c}C_{m_{\delta_e}} & 0 \\ bC_{n_{\delta_a}} & 0 & bC_{n_{\delta_r}} \end{bmatrix} \tag{5}$$

Equations 4 and 5 can be incorporated in the rotational dynamics of rigid-body aircraft over a flat non-rotating earth as given in the Newton-Euler equation (Equation 6), where J is the inertia tensor as given in Equation 7. This leads to Equation 8.

$$\dot{\boldsymbol{\omega}} = \boldsymbol{J^{-1}}(\boldsymbol{M_A} + \boldsymbol{M_T} - \boldsymbol{\omega} \times \boldsymbol{J\omega}) \tag{6}$$

$$\boldsymbol{J} = \begin{bmatrix} I_{xx} & 0 & -I_{xz} \\ 0 & I_{yy} & 0 \\ -I_{xz} & 0 & I_{zz} \end{bmatrix} \tag{7}$$

$$\dot{\boldsymbol{\omega}} = \boldsymbol{J^{-1}}(\boldsymbol{M_a} + \boldsymbol{M_c u} - \boldsymbol{\omega} \times \boldsymbol{J\omega}) \tag{8}$$

The control law for INDI is obtained by taking a first-order Taylor expansion around the current point in time, which is denoted by the subscript 0. This Taylor expansion can be found in Equation 9.

$$\begin{aligned} \dot{\boldsymbol{\omega}} \approx \dot{\boldsymbol{\omega}}_{\mathbf{0}} &+ \frac{\partial}{\partial \boldsymbol{\omega}} \left(\boldsymbol{J^{-1}}(\boldsymbol{M_a} + \boldsymbol{M_c u} - \boldsymbol{\omega} \times \boldsymbol{J\omega}) \right) (\boldsymbol{\omega} - \boldsymbol{\omega}_{\mathbf{0}}) \\ &+ \frac{\partial}{\partial \boldsymbol{u}} \left(\boldsymbol{J^{-1}}(\boldsymbol{M_a} + \boldsymbol{M_c u} - \boldsymbol{\omega} \times \boldsymbol{J\omega}) \right) (\boldsymbol{u} - \boldsymbol{u}_{\mathbf{0}}) \end{aligned} \tag{9}$$

Downloaded by TU DELFT on January 6, 2020 | http://arc.aiaa.org | DOI: 10.2514/6.2020-0852

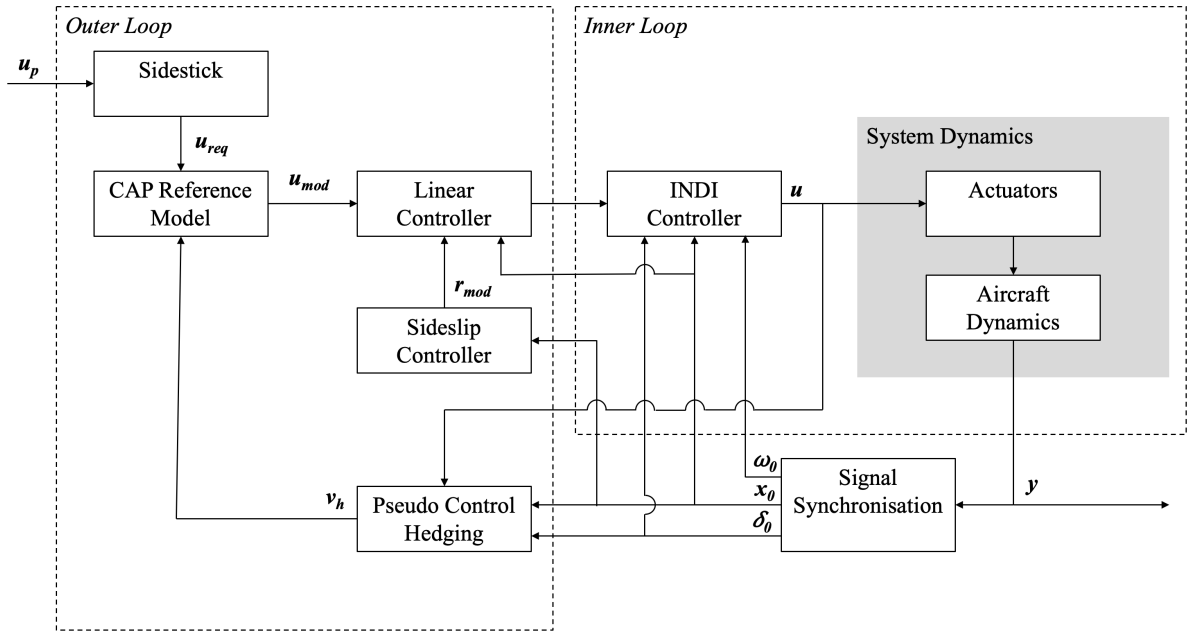

Fig. 1 Schematic block diagram of the controller structure

The controller runs at 1,000 Hz, thus the time increments are relatively small. This fact, combined with assuming instantaneous control effectors ($\omega - \omega_0 \ll u - u_0$) and assuming that $\omega - \omega_0 = 0$, leads to a simplification of Equation 9 to Equation 10, where $\Delta u = u - u_0$:

$$\dot{\omega} \simeq \dot{\omega_0} + J^{-1} M_c \Delta u \tag{10}$$

Inversion of Equation 10 leads to the INDI control law as implemented in the controller. This results in Equation 11, where the input of the linear controller v_e replaces $\dot{\omega}$ and the current control surface deflections δ_0 are added. A schematic overview is given in Figure 2.

$$u = M_c^{-1} J (v_e - \dot{\omega_0}) + \delta_0 \tag{11}$$

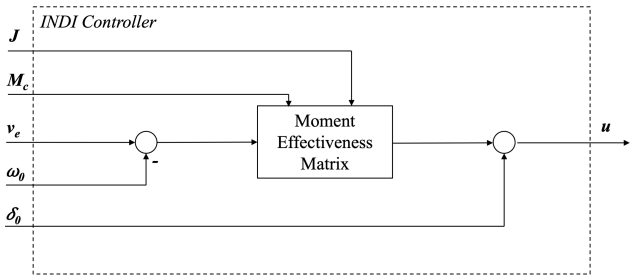

Fig. 2 Schematic block diagram of the INDI controller

2. System Dynamics

The system dynamics are based on the DASMAT model of the Cessna Citation 500 described by Borst [30]. Although developed for another variant, the DASMAT model is preferred over the newer Cessna Citation II model developed by Van den Hoek et al. [31], since it also includes models for the moments of the trim tabs. These moments are relevant when the model has to be trimmed towards steady, straight flight with the lowest possible hinge moment in the elevator. This low hinge moment in the elevator is required to maximise the performance of the limited fly-by-wire system.

The non-linear actuator model from Lubbers [14] is implemented in this DASMAT model. An alternative to this non-linear actuator model is based on a first-order approximation performed by Grondman et al. [13]. To be able to use both the non-linear actuator model and a more basic approximation of the actuators, both are modelled and a switch is added to select the used model. Grondman's model has been extended to make use of the saturation flags from the full actuator model by Lubbers [14], to ensure the appropriate saturation deflections.

During the flight test experiment, the DASMAT model is still used to determine the moment induced by the control effectors. However, the mass model has been updated to include the appropriate inertias and masses from the Citation II. The outputs from the aircraft sensors are synchronised and filtered using basic first-order low-pass filters, except for the angular acceleration which is filtered using a second-order low-pass filter ($\omega = 20$ [*rad/s*] and $\zeta = 1$). These outputs are used in the remainder of the controller.

Downloaded by TU DELFT on January 6, 2020 | http://arc.aiaa.org | DOI: 10.2514/6.2020-0852

C. Outer Loop

1. Sideslip Controller

The Cessna Citation II fly-by-wire hardware does not include a yaw input device, which means that coordinated flight can only be achieved when the sideslip is controlled. This has been recognised by Grondman et al. [13], who developed a PI controller to control the sideslip to zero. This is described in Equation 12, where $K_\beta = 1.93$, $K_{\beta_I} = 0.977$ and $w = V_{tas} \sin\alpha \approx V_{tas}\alpha$.

$$r_{mod} = \frac{1}{V_{tas}} \left(wp - f_y\right) \left(\frac{1}{s} K_{\beta_I}(\beta_{cmd} - \beta) - K_\beta \beta\right) \tag{12}$$

2. Pseudo-Control Hedging

Johnson and Calise [32] developed a technique to compensate for actuator limitations by modifying the reference model dynamics. This technique is called Pseudo-Control Hedging (PCH). PCH is implemented in the controller to compensate for actuator saturation, which is expected due to the limited fly-by-wire system performance. PCH uses the inverse of the moment effectiveness matrix to correct for the differences between the commanded deflection by the INDI controller and the actual deflection of the actuators. This provides the hedging signal as indicated in Equation 13:

$$\boldsymbol{v_h} = \boldsymbol{M_c J^{-1}}(\boldsymbol{u} - \boldsymbol{\delta_0}) \tag{13}$$

Looye et al. [33] activated the PCH only when saturation occurred, whilst Grondman et al. [13] always kept the PCH active. In the latter case, the reference logic is also corrected for limited actuator speed instead of only the actuator position and this option is therefore preferred.

3. CAP Reference Logic

The CAP reference logic in pitching motion is designed to ensure a requested CAP and damping using the second order approximation as determined by Bischoff [26]. The linear controller uses $\boldsymbol{u_{mod}}$ as an input, which is essentially a reference pitch and roll rate. Yaw is not controlled to zero by the controller, thus it is not present in the CAP reference logic. To convert the requested input $\boldsymbol{u_{req}}$ to these reference rates, an estimation of both the pitch gain K_θ and the longitudinal coefficient T_{θ_2} are required as given in Equation 2. To achieve this estimation, the method from Morelli [29] is used. Since the CAP and damping are design parameters, Equation 2 can be rewritten to provide the final CAP reference model, Equation 14, with the corresponding coefficients in Equation 15.

$$\frac{u_{mod_q}}{u_{req_q}} = \frac{a_1 s + a_2}{s^2 + b_1 s + b_2} \tag{14}$$

$$\begin{aligned} a_1 &= K_\theta & a_2 &= \tfrac{K_\theta}{T_{\theta_2}} \\ b_1 &= 2\zeta_q \sqrt{\mathrm{CAP} \cdot \tfrac{V}{g} \tfrac{1}{T_{\theta_2}}} & b_2 &= \tfrac{\mathrm{CAP}}{T_{\theta_2}} \tfrac{V}{g} \end{aligned} \tag{15}$$

In rolling motion, different reference dynamics are used as given in Equation 16, with the coefficients defined as in Equation 17. Grondman et al. [13] performed a design optimisation for these coefficients, resulting in $\zeta_p = 1$ and $\omega_p = 1.35$ [*rad/s*].

$$\frac{u_{mod_p}}{u_{req_p}} = \frac{c_1}{s^2 + d_1 s + d_2} \tag{16}$$

$$c_1 = \omega_p^2 \quad d_1 = 2\zeta_p \omega_p \quad d_2 = \omega_p^2 \tag{17}$$

4. Sidestick

The inputs from the pilot have to be scaled before they can enter the controller. Since both roll and pitch axes have different reference logic, they need different gains. The initial values were determined using a pilot model, where the gain was changed until the open loop crossover frequency ω_c was equal to 2 [*rad/s*]. This led to the following standard stick gains: Pitch $K_q = 0.0125$ and roll $K_p = 0.65$.

5. Linear Controller

The linear controller was designed to follow the reference model as closely as possible. For the pitch and roll channel, the error for the state and the first derivative are controlled. In addition, a feedforward gain was added to the second derivative. The result can be seen in Equations 18-19:

$$v_{\dot\phi} = \left(K_\phi + \frac{K_{\phi_I}}{s}\right)(u_{mod_p} - \phi) + K_{\dot\phi}(\dot u_{mod_p} - \dot\phi) + K_{\ddot\phi}\ddot u_{mod_p} \tag{18}$$

$$v_{\dot\theta} = \left(K_\theta + \frac{K_{\theta_I}}{s}\right)(u_{mod_q} - \theta) + K_{\dot\theta}(\dot u_{mod_q} - \dot\theta) + K_{\ddot\theta}\ddot u_{mod_q} \tag{19}$$

Sideslip is controlled in the yaw channel, without any pilot input:

$$v_r = K_r(r_{mod} - r) \tag{20}$$

Grondman et al. [13] performed a robust parameter synthesis to optimise these gains. However, their design requirements were different, since they did not require exact model-following. A linear parameter grid search was performed to find the combination of gains that enabled better model-following performance. The results of this analysis are summarised in Table 1.

IV. Offline Simulation

Multiple offline simulations were performed to investigate the performance of the controller. In addition, the offline simulations were used to determine the optimal flight condition considering the moment effectiveness and actuator saturation. This led to an initial estimation of the system limitations.

Downloaded by TU DELFT on January 6, 2020 | http://arc.aiaa.org | DOI: 10.2514/6.2020-0852

Table 1 Linear controller gains

Roll		*Pitch*	
K_{ϕ}	5.51	K_{θ}	7.76
K_{ϕ_I}	1.34	K_{θ_I}	0.50
$K_{\dot{\phi}}$	4.80	$K_{\dot{\theta}}$	4.80
$K_{\ddot{\phi}}$	1.05	$K_{\ddot{\theta}}$	0.70
Yaw			
K_r	1.62		

A. CAP and damping performance

To investigate the performance in placing the CAP and damping parameters, step inputs were given on the pitch axis in Figure 3. The same step input is given in both situations, but the settings for the CAP reference model are different. Figure 3a shows the response of the aircraft for a CAP of 0.6 and a damping of 1.0. Figure 3b depicts the response for a CAP of 1.1 and a damping of 0.3. It can be seen that the controller modifies the response of the elevator to match the requested dynamics as closely as possible. In both cases the PCH is enabled, which results in the difference between the commanded signal and the reference signal.

The matching performance of the PCH depends on a proper synchronisation of the signals. A transport lag exists between the commanded deflection and the actual deflection of the actuators, which resulted in an over-correction by the hedging signal. During the offline simulations and the fixed-base experiment this transport lag is relatively constant, but in real flight this lag may vary due to various non-linearities. In addition, the hedging signal directly adapts the CAP reference logic. This implies that the handling qualities change when PCH is enabled, which is undesired behaviour. This should be taken into account when using PCH in the flight tests.

B. Flight condition

The offline model was used to investigate the initial flight condition that would result in the highest pitch and roll rates. This condition was limited by two main factors, being the moment effectiveness and the deflection of the actuators. The moment effectiveness is higher for high speeds and low altitudes, whereas the maximum deflection of the actuators is higher at low speeds and high altitudes. A controller in the fly-by-wire system allows command over the deflection angle of the control surfaces, by controlling the servo motor position. The transmission ratio between deflection of the control surface and position of the servo motor is not a fixed ratio, however. It is a function of the force on the actuator cables due to cable stretch. The control effectiveness therefore changes dependent on the flight condition. Combining these factors led to an initial condition of $4,000$ $[m]$ altitude and a true airspeed of 110 $[m/s]$. At altitudes higher than approximately $4,250$ $[m]$, torque limiters are active for the fly-by-wire system. This was one of the main limiting factors when determining the optimal initial condition with respect to system performance.

C. System limit prediction

To determine the CAP and damping limits of the system, it is necessary to make an assumption regarding the time it takes before pilots experience differences in handling qualities due to actuator saturation. In addition, this is dependent on the behaviour of the pilot during the experiment. Some pilots might fly the aircraft with a higher gain, which results in different crossover frequencies and actuator use. The effect of both parameters on the system limits is investigated. It was found that the crossover frequency has a considerable impact on the system limits. This is due to the actuator saturation that occurs more frequently and for a prolonged time when the crossover frequency is higher. For the initial system limit prediction it is assumed that pilots feel a difference in handling qualities when actuator saturation of 0.2 seconds or longer occurs. This assumption will be updated after the simulator experiment, since this gives an opportunity to investigate a relation between experienced handling qualities and the actuator saturation.

Using a pilot model with different crossover frequencies it was investigated for which combinations of CAP and damping actuator saturation of 0.2 seconds would occur for the control task of the fixed-base simulator experiment. Figure 4 illustrates the effect of two different crossover frequencies as a function of CAP and damping ratio for the defined control task. The pink dots represent the initial conditions chosen for the simulator experiment, which will be explained in more detail below.

V. Experiment 1: Fixed-base Simulator

A fixed-base simulator experiment is performed to investigate what the system limits are due to the actuator saturation for a specific control task. In addition, it is investigated whether pilots can feel the difference between simulating just the reference model, and simulating the complete non-linear dynamics of the reference model, controller and aircraft.

A. Method

1. Apparatus

The experiment was performed in a fixed-base, part-task flight simulator at Delft University of Technology's Human Machine Interaction Laboratory (HMI lab). Figure 5 depicts the layout of the aircraft configuration. It consists of an adjustable aircraft seat, two 18 inch LCD panels that show the instrumentation and three DLP projectors which are used to display the outside visuals. Participants used an electrohydraulic sidestick to control the motion in pitch and roll. Clouds were added to the simulation to enhance the experience of forward motion for the pilots.

2. Software

Since multiple experiments were performed on different platforms, DUECA is used as the main software platform [34]. DUECA has been developed to act as a middleware layer between hardware (simulators/research aircraft) and the actual control software itself. It is able to synchronise data from

Downloaded by TU DELFT on January 6, 2020 | http://arc.aiaa.org | DOI: 10.2514/6.2020-0852

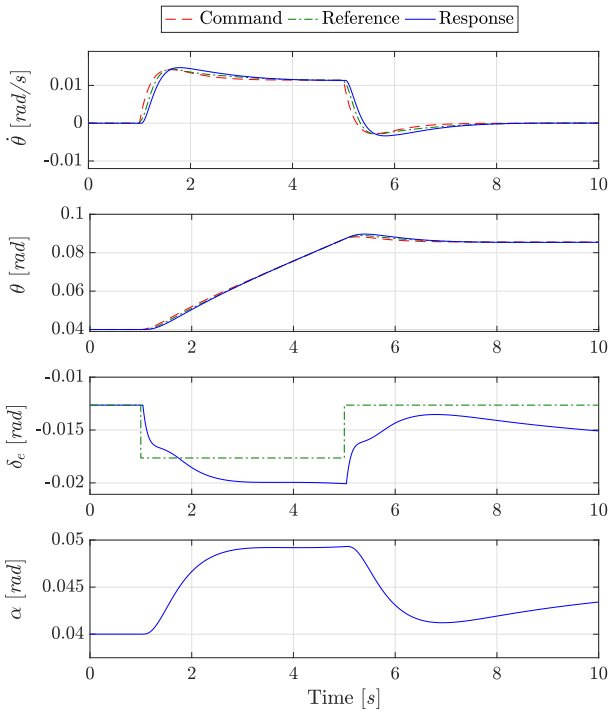

(a) CAP = 0.6; Damping = 1.0

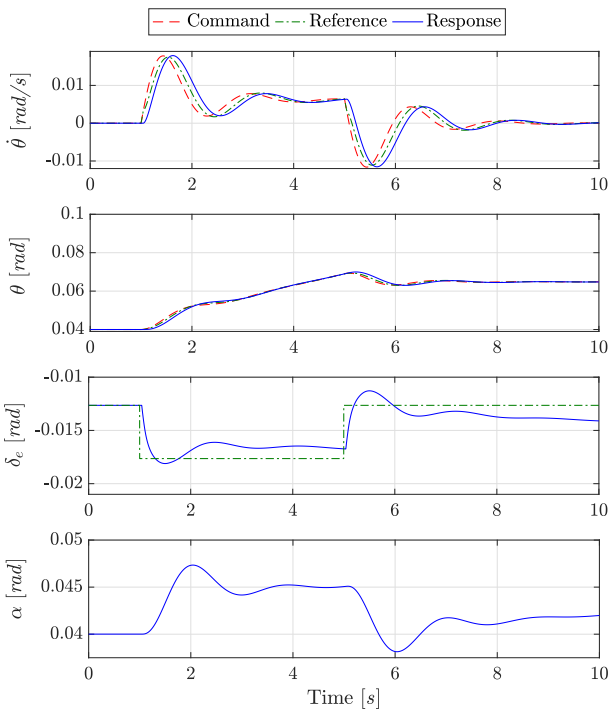

(b) CAP = 1.1; Damping = 0.3

Fig. 3 Aircraft pitch response for different CAP and damping values, with PCH enabled

different sources and it combines processes that are running at different frequencies. Different modules can be selected within the software, which makes the implementation on different platforms easier. In addition, controllers developed in the MATLAB/Simulink environment are easily converted and implemented to control either the simulators or the Cessna Citation II laboratory aircraft.

3. Subjects and Instruction to Subjects

Eight pilots participated in the experiment (Table 2). They were instructed to control the aircraft's rate of climb to $1,000$ [*feet/min*] and $-1,000$ [*feet/min*], with a performance band around the commanded rate of climb of 10%. Every ten seconds they were commanded to switch between ascent and descent.

4. Independent Variables

The experiment had one independent variable: the model that the pilot is using to fly the simulation. Two models were flown: the reference model and the full model. The reference model (CAPR) uses the response from the CAP reference model and sends these dynamics directly to the simulator. The full model (FULL) also includes the controller and the aircraft dynamics. This is represented in the block diagram in Figure 6. The CAP reference model is not limited by actuator saturation, whereas the full model includes these limitations.

Table 2 Characteristics of the pilot subjects

Pilot	Age	Gender	Hours	Types of aircraft
A	52	M	12,000	Single engine; B777; B787; Cessna Citation II (1,000h)
B	63	M	20,000	Single engine; B777; B787; Cessna Citation I (500h)
C	59	M	3,700	Single engine; F5; F16
D	65	M	22,000	Single engine; B737; B747; Cessna Citation I (50h)
E	42	M	3,700	Single engine; Cessna Citation II (1,650h)
F	46	M	2,200	Single engine; SA266/277; Cessna Citation II (1,300h)
G	58	M	14,300	Single engine; Jet engine; Cessna Citation II (3,000h)
H	52	M	1,300	Single engine; Jet engine; Cessna Citation II (6h)

5. Experimental Design and Procedure

The experiment was designed to be full-factorial within-subjects. The CAP conditions were selected to ensure that different system limitations, due to actuator saturation, could be experienced. This resulted in a CAP of 0.90, 0.45 and 0.25.

The different damping conditions were selected to have all three levels of acceptability in the experiment. The original

Downloaded by TU DELFT on January 6, 2020 | http://arc.aiaa.org | DOI: 10.2514/6.2020-0852

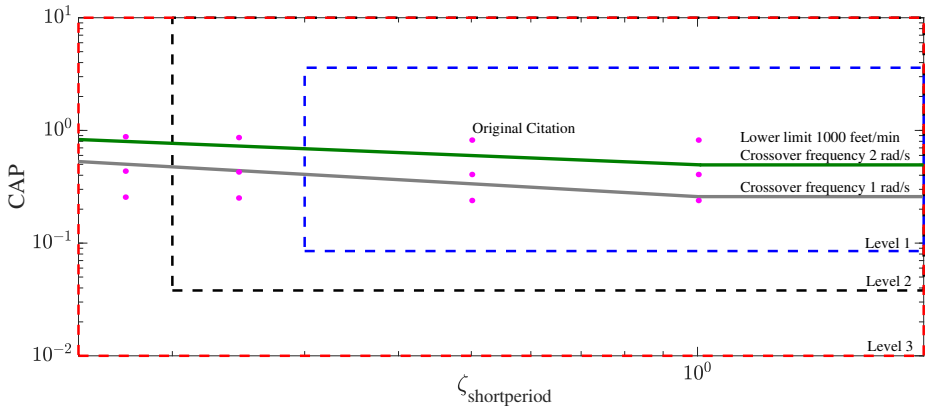

Fig. 4 Initial conditions displayed with predicted limitations from offline simulation

Fig. 5 Fixed-base simulator in aircraft configuration

damping of the Cessna Citation II was also included and this resulted in a damping of 0.15, 0.25, 0.5 and 1.0. Combined with the initial CAP conditions, this yielded 12 conditions which are represented by the pink dots in Figure 4.

The initial conditions were flown for both the CAP reference model and the full model, resulting in a total of 24 runs. The 24 runs were divided into 4 sets of 6 runs, where for every set the damping coefficient remained constant, whilst the CAP and simulation model varied. Before every set, training runs were performed to suppers learning effects. These training runs were performed on the settings of the first run of the upcoming set. An example experiment schedule, for one pilot, is shown in Table 3. Sets were varied over all pilots, including the start with the full or CAP reference model per set. The resulting experiment matrix required eight pilots. The initial flight conditions of all runs were defined according to the offline simulation (4, 000 [m] altitude and 110 [m/s] true airspeed).

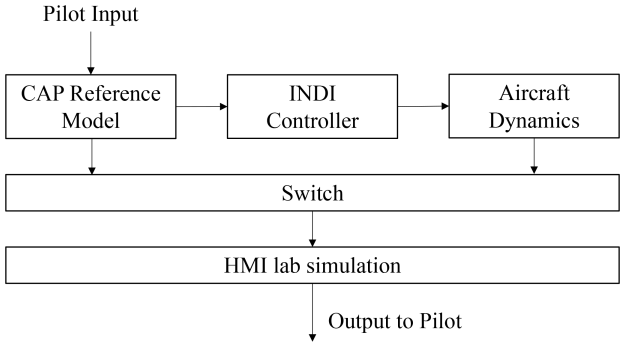

Fig. 6 Flow diagram concerning the independent variable with two conditions

6. Dependent Measures

The dependent measures are used to determine the differences between the conditions of the independent variable. In addition, they are also used to find the limits of the full model based on actuator saturation. The dependent measures are defined as follows:

- **Cooper-Harper Rating Scale:** The subjects had to give a Cooper-Harper rating after every run. The difference between the CAP reference model and the full model for the same initial condition is used to compare the results.
- **Performance:** The total time spent within the specified 10% bandwidth around the required rate of climb is used as performance indicator. The percentage of the total run time is referred to as the performance ratio.
- **Control activity:** An increased workload indicates that the pilot has a harder time flying the aircraft. The control activity during the simulation may therefore be used as workload measure. Control activity is measured by the variance of the input of the pilot. Since the main goal is to determine whether the pilots notice the change in longitudinal handling qualities, only the control activity in pitch is of interest.
- **Actuator saturation:** Actuator saturation is measured

Downloaded by TU DELFT on January 6, 2020 | http://arc.aiaa.org | DOI: 10.2514/6.2020-0852

Table 3 Example of an experiment schedule for one pilot

SET 1	SET 2	SET 3	SET 4
Damp 0.15	Damp 0.25	Damp 0.50	Damp 1.0
CAPR	FULL	CAPR	FULL
CAP 0.9	CAP 0.9	CAP 0.9	CAP 0.9
FULL	CAPR	FULL	CAPR
CAP 0.9	CAP 0.9	CAP 0.9	CAP 0.9
FULL	CAPR	FULL	CAPR
CAP 0.45	CAP 0.45	CAP 0.45	CAP 0.45
CAPR	FULL	CAPR	FULL
CAP 0.45	CAP 0.45	CAP 0.45	CAP 0.45
CAPR	FULL	CAPR	FULL
CAP 0.25	CAP 0.45	CAP 0.25	CAP 0.25
FULL	CAPR	FULL	CAPR
CAP 0.25	CAP 0.45	CAP 0.25	CAP 0.25

since a correlation is expected between the actuator saturation and the differences in Cooper-Harper rating between the different models. Two different flags are used. The first one is logged when actuator saturation occurs and will be referenced as *saturation flag* in the remainder of this paper. The second one is logged when actuator saturation occurs *and* the requested input of the pilot is in the opposite direction of the current aircraft movement. In other words, a pilot might not feel saturation when the aircraft is moving in the direction as requested by the pilot. This flag is referenced to as the *combined flag*.

7. Experiment hypotheses

It is hypothesised that:

- **H.1:** Pilot performance is similar for both models if no actuator saturation is occurring. Performance is expected to be lower if pilots reach the saturation limits of the actuators. Since actuator saturation is expected during the experiment, the full model is likely to have lower performance compared to the CAP reference model.
- **H.2:** The control activity is higher for the full model, since the full model includes actuator saturation. This means that pilots will sometimes not experience the expected response from the aircraft.
- **H.3:** Pilots will give more similar Cooper-Harper ratings for a higher CAP, since the offline simulation showed that actuator saturation time is lower for these conditions. However, this depends on the crossover frequency of the pilot and the assumption that pilots only experience differences when a saturation time of more than 0.2 seconds occurs.

B. Results

1. Cooper-Harper difference

The difference in Cooper-Harper rating between both models is displayed in Figure 7. It can be seen that most runs were assessed with two points difference, which means that pilots experience the full model to have a worse rating compared to the CAP reference model. For only one run the full model was considered to be the better model. There was a statistically significant difference in Cooper-Harper rating depending on the initial CAP level, $\chi^2(2) = 44.816$, $p < 0.00$. Post hoc analysis was performed using the Wilcoxon signed-rank tests with a Bonferroni correction (significance level of $p < 0.02$). Median perceived Cooper-Harper differences for the CAP of 0.90, 0.45 and 0.25 were 1 (0 to 2), 2 (2 to 4) and 2 (2 to 3.75), respectively. There were significant differences between the CAP 0.90 and 0.45 condition ($Z = -4.247$, $p < 0.00$) and between the CAP of 0.90 and 0.25 ($Z = -4.430$, $p < 0.00$). However, there was no statistically significant reduction in the perceived Cooper-Harper difference between CAP 0.45 and 0.25 ($Z = -0.540$, $p < 0.59$).

The difference in rating can be illustrated using the aircraft response of two experiment runs. Figure 8 shows a run of the full model, where the pilot did not notice any differences compared to the CAP reference model (0 point Cooper-Harper difference). The first subplot shows the rate of climb and the performance bands (marked as two grey boxes). Furthermore, the pitch angle and elevator deflection are given. Finally, the pilot input is displayed. It can be seen that the longest sustained saturation time occurs in the black dotted box between 80 and 90 seconds (the previously mentioned saturation flag). Even though the model is experiencing saturation, the pilot still graded the full model similar to the CAP reference model.

Figure 9 shows another run of the full model, but here the pilot is noticing a six-point Cooper-Harper rating difference with respect to the CAP reference model. Saturation occurs more often and is sustained for a longer period of time. Like before, the black dotted box between 40 and 50 seconds shows the saturation flag. The magenta box shows the combined flag, during which the pilot tries to steer the aircraft in a different direction, but the aircraft does not respond as requested.

The maximum saturation time for both the saturation flag and the combined flag can be plotted against the Cooper-Harper differences. This can be used to investigate the correlation between the maximum flag time and the difference in experienced handling qualities. The saturation flag is plotted in Figure 10, whereas the combined flag is displayed in Figure 11. The digit behind the summation symbol Σ represents the number of data points in the respective column. It can be seen that the flag time means and standard deviations increase when the perceived Cooper-Harper rating difference increases. The saturation flag appears to have higher means compared to the combined flag. However no statistically significant linear correlation could be found between the Cooper-Harper differences and their corresponding maximum flag time.

Downloaded by TU DELFT on January 6, 2020 | http://arc.aiaa.org | DOI: 10.2514/6.2020-0852

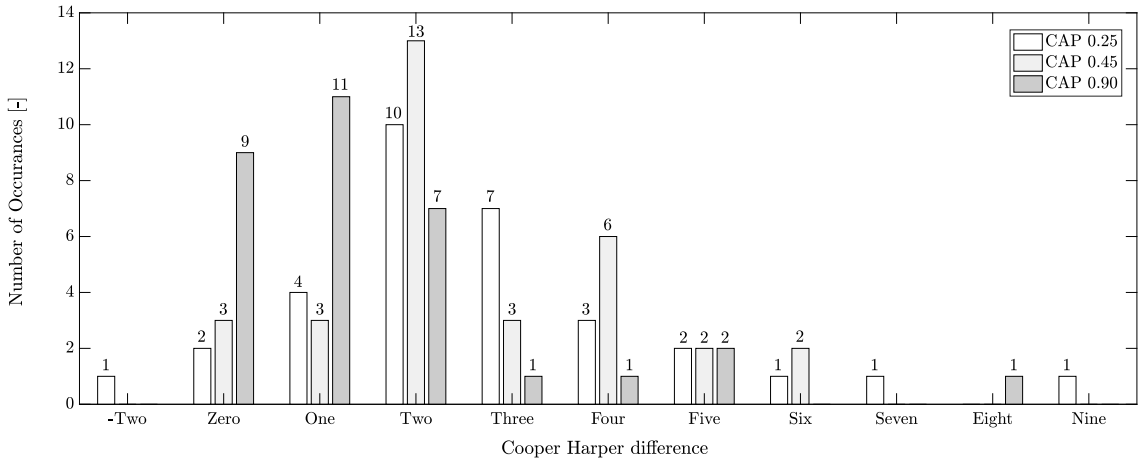

Fig. 7 Cooper-Harper difference between CAP reference model and the Full model as indicated by the pilots

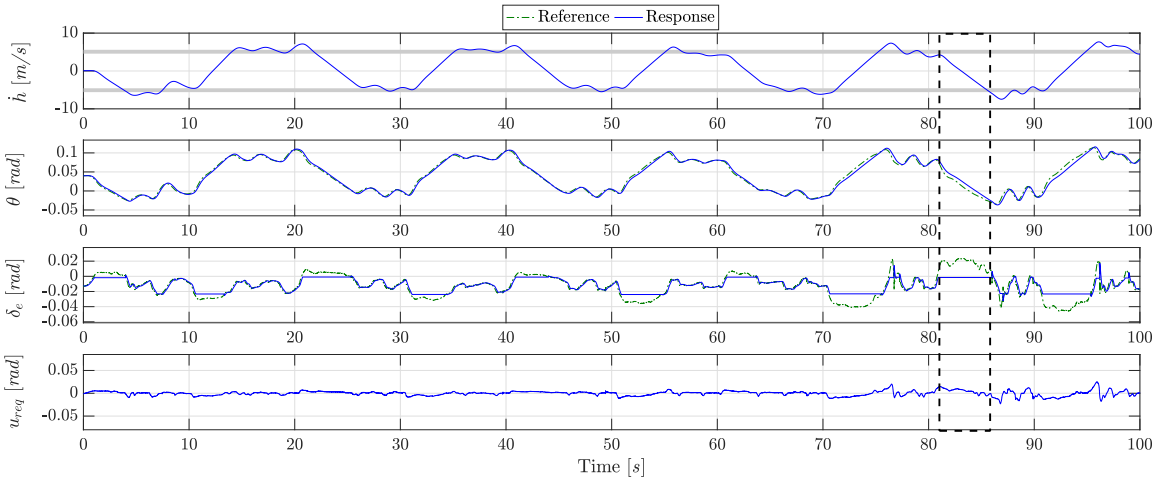

Fig. 8 Aircraft response with Cooper-Harper difference of 0pt (CAP 0.9; Damping ratio 0.25)

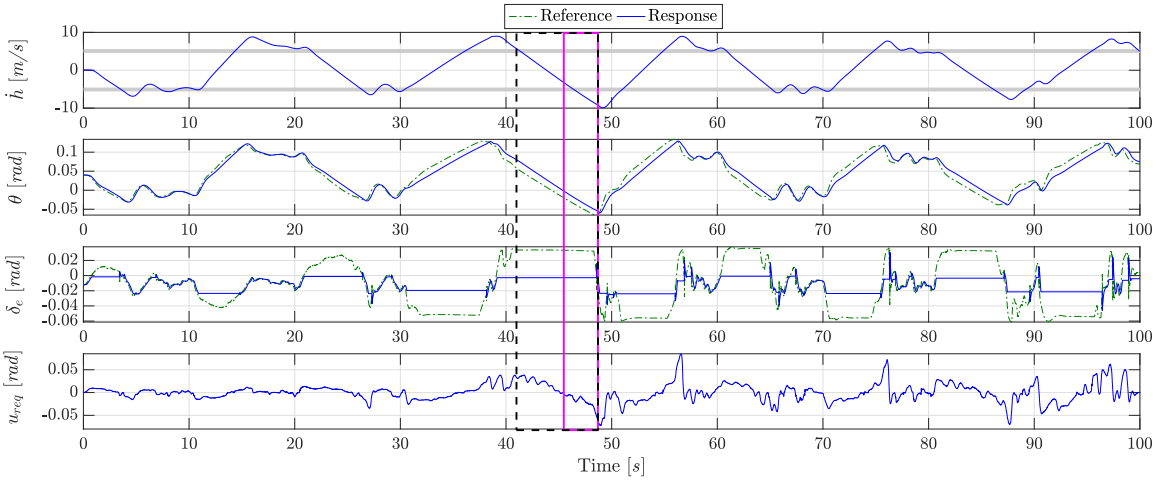

Fig. 9 Aircraft response with Cooper-Harper difference of 6pt (CAP 0.25; Damping ratio 1.0)

Downloaded by TU DELFT on January 6, 2020 | http://arc.aiaa.org | DOI: 10.2514/6.2020-0852

Downloaded by TU DELFT on January 6, 2020 | http://arc.aiaa.org | DOI: 10.2514/6.2020-0852

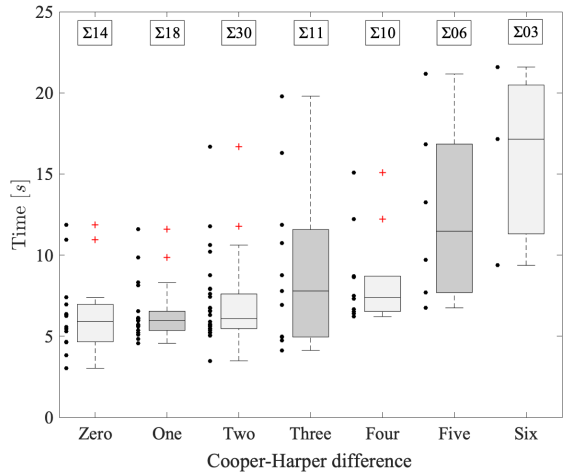

Fig. 10 Means and the 95% confidence limits of the saturation flag sorted by Cooper-Harper difference

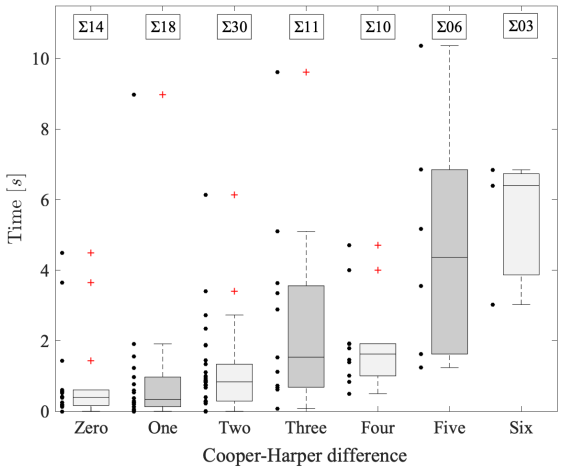

Fig. 11 Means and the 95% confidence limits of the combined flag sorted by Cooper-Harper difference

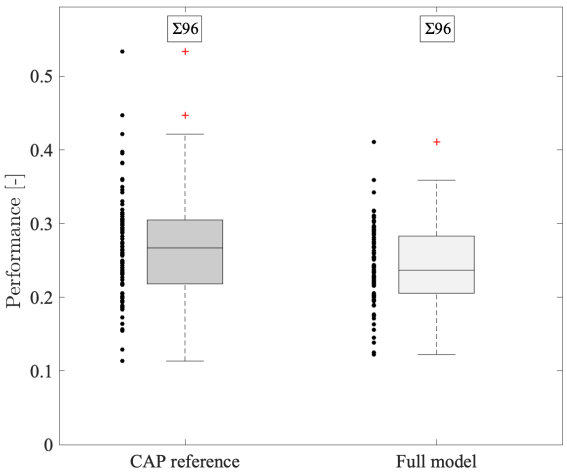

Fig. 12 Means and the 95% confidence limits of the performance

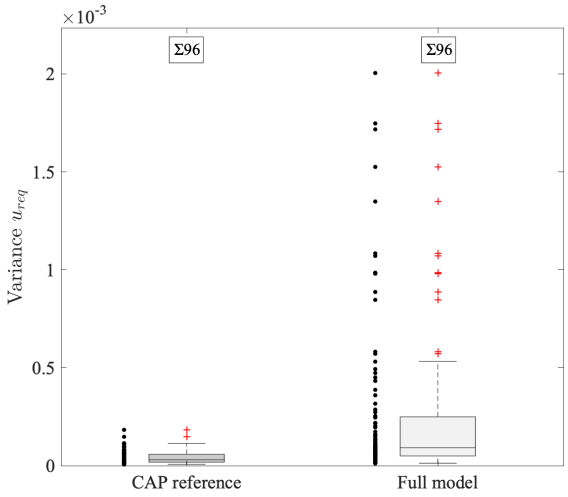

Fig. 13 Means and the 95% confidence limits of the control activity

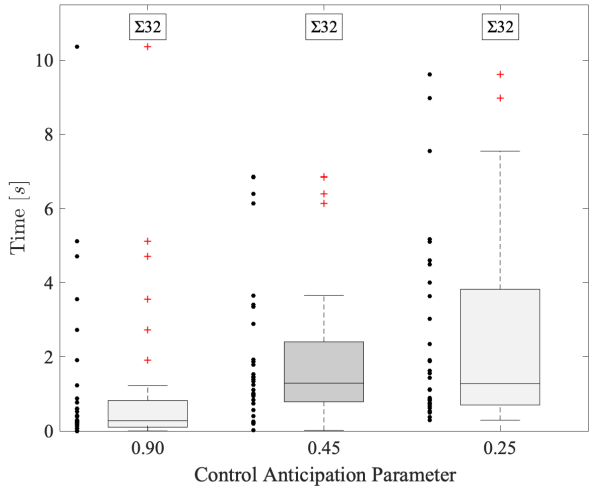

Fig. 14 Means and the 95% confidence limits of the combined flag sorted by CAP

2. Statistical Analysis of other dependent measures

Performance of the test subjects using both models is shown in Figure 12. Since the data passed the normality and homogeneity of variance tests, a dependent t-test is performed to evaluate differences. Performance in the full model (0.242 ± 0.052) was significantly lower compared to the CAP reference model (0.268 ± 0.070) with $t(95) = 3.387$ and $p < 0.05$.

Control activity of test subjects using both models is shown in Figure 13. The control activity data did not pass the normality and homogeneity of variance tests. A Wilcoxon signed-rank test is therefore applie to compare the results. This test showed a statistically significant lower control activity with the CAP reference model ($Z = -8.018$ and $p < 0.00$).

The combined flag duration is illustrated in Figure 14, as function of CAP levels. Mauchly's test $\chi^2(2) = 6.225, p < 0.04$ indicates that the assumption of sphericity is violated. Using a full-factor ANOVA and applying a Greenhouse-Geisser correction determined that the mean CAP differed significantly ($F_{1.684} = 6.831, p < 0.00$). Post hoc tests with Bonferroni correction (significance level of $p < 0.02$) show that the CAP of 0.90 (1.129 ± 2.15) differs significantly from the CAP of 0.25 (2.456 ± 2.54) $p < 0.01$, but there are no significant differences between a CAP of 0.90 and 0.45 (1.964 ± 1.993) $p < 0.03$ and a CAP of 0.45 and 0.25 with $p < 0.49$. However, the difference between a CAP of 0.90 and 0.45 is close to the significance level of $p < 0.02$.

C. Discussion and conclusions

The purpose of the simulator experiment was to identify whether pilots could notice the difference in handling qualities between the CAP reference logic and a full aircraft dynamic model including the controller.

The first hypothesis (H.1) is confirmed, since the performance of the pilots was lower for the full model compared to the CAP reference model. When actuator saturation is occurring, it is more difficult for pilots to achieve desired performance.

H.2 is also confirmed. The control activity of the pilots was indeed higher for the full model compared to the CAP reference model. This can be explained by the additional control efforts of pilots that occur when the aircraft does not respond according to their expectations, here mostly due to actuator saturation.

The full model is generally rated at a lower Cooper-Harper rating compared to the CAP reference model. This relates to the difference in response between the models in case of actuator saturation. In addition, some lag is present within the full model due to the actuator dynamics (requested deflection by the pilot is not instantly the actual deflection), whereas this lag is not present in the CAP reference model. At CAP values of 0.90 the mean difference between the experienced handling qualities was on average only 1 Cooper-Harper rating point, whereas this difference increased for lower CAP values with increased actuator saturation. This confirms H.3, since the model mismatch was higher for CAP below the lower limits determined in offline simulation.

It was investigated how long the saturation time would be before the pilots experienced different handling qualities. However, differences in Cooper-Harper rating appear not to be directly related to the flag time. Additional runs would be required to investigate this in more detail. The lower limits obtained with the offline simulations (Figure 4) are updated with the acquired saturation time information as shown in Figure 15. The updated estimation includes the expected Cooper-Harper differences for specific CAP and damping settings for this control task. The updated simulation model can be used for different control tasks to investigate the limits of the full system.

VI. Experiment 2: Flight Test

To validate the controller design and implementation, four flight tests were performed over the course of eight days. The flights all departed from and terminated at Amsterdam Schiphol Airport (AMS) and were flown in the TMA Delta and above the North Sea, within the Netherlands Airspace. The system is validated using the three initial flight tests, whereas the final flight was a demonstration flight.

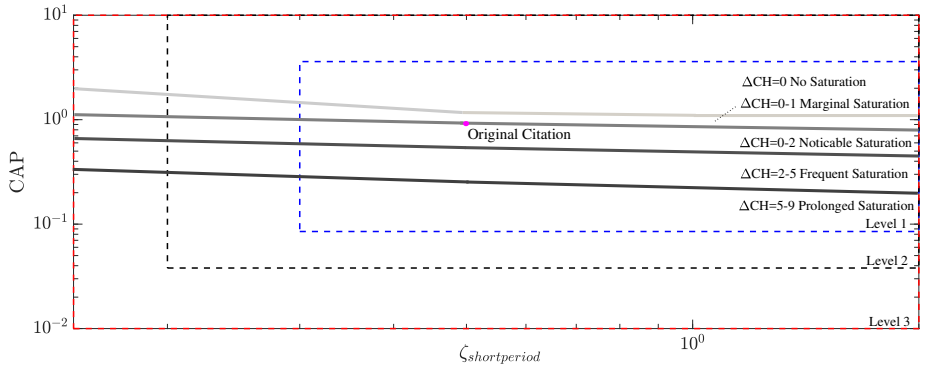

Fig. 15 Updated handling quality limitations using the combined flag saturation information

Downloaded by TU DELFT on January 6, 2020 | http://arc.aiaa.org | DOI: 10.2514/6.2020-0852

A. Method

1. Apparatus

The Cessna Citation II laboratory aircraft, jointly operated by TU Delft and the Netherlands Aerospace Centre, was used in the flight tests. The flight tests are performed in a clean configuration with spoilers, gear and flaps retracted. The angle of attack and side slip are measured in clean air using a boom mounted in front of the aircraft. Activation of the automatic trim would disrupt the experimental control system, therefore the trim was deactivated. The aircraft was controlled by the co-pilot, sitting on the right-hand side, using force input on a side-stick. The captain acted as the safety pilot. The experimenter controlled the software and its variable stability settings via a wireless connection using a laptop in the cabin.

2. Changes to controller

Multiple changes were made to the controller with respect to the simulator version. The citation model system dynamics were modified to follow the state give by flight measurements and changed to ensure that they only output the moment effectiveness matrix. All other outputs were received from sensors based on the aircraft itself. The requested deflection that comes from the INDI controller was linked to the autopilot servos from the existing aircraft fly-by-wire system [15].

New angular accelerometers were installed on the Cessna Citation II laboratory aircraft. These were an addition to the previously available angular accelerations which were established by differentiating the angular rates. Second order filters were introduced to these angular accelerations to remove noise whilst still maintaining the original signal without too much lag.

The controller required a conversion of the stick gains, since the stick on the aircraft was not identical to the electro-hydraulic stick used in the simulator. The stick on the aircraft converted the input from the pilots to a different scale, thus the gains were adapted to maintain the same scaling (in command input per stick force) as in the simulator.

In comparison to the fixed initial conditions in the fixed-based simulator, the initial conditions depend on the actual flight conditions upon experiment initiation. The updated initial conditions were also used in the determination of the moment effectiveness matrix.

The fixed-base simulator experiment was based on the DASMAT model, which consisted of an inertia tensor based on the Cessna Citation I. Since the experiment is conducted in the Cessna Citation II, it was required to update this inertia tensor based on the newly developed model by Van den Hoek et al. [31]. The model mismatch between the DASMAT model and the new model was highest for the inertia around the y-axis I_{yy}, with a 35% change. The I_{xx}, I_{zz} and I_{xz} showed an increase of 8%, 24% and 27%, respectively.

3. Procedure

The experiments in pitch focused mainly on the longitudinal handling qualities, similar to the experiment in the simulator. In addition, a number of roll manoeuvres were performed to test the differences in roll time constants. To demonstrate the system potential to be used in pilot training, the effects of roll time constants, stick time delays and stick gains were also investigated.

Two initial conditions were used during the different flight tests. Both conditions were at an altitude of FL130, but with a varying airspeed of 175 or 190 knots. To ensure safe execution of the experiment, the following procedure was used during the experiments. First, the safety pilot flew to the requested altitude. Then he trimmed the aircraft for the desired airspeed in horizontal flight and disabled the auto trim. At the same time, the experimenter selected the desired parameter configuration in the DUECA software. Activation of the autopilot based on the controller software required activation of both the roll and pitch axes. This was achieved by a trigger of both the safety pilot and the experimenter, for each axis. Finally, the experimental control mode was initiated by the co-pilot, with "hands-off-stick" to prevent undesirable initial control inputs.

4. Subjects and Instruction to Subjects

To validate the controller by noticing the differences in handling qualities, pilots require experience on the Cessna Citation II laboratory aircraft. Three pilots have flown the aircraft in the experiments, being pilots E, F and G (Table 2). In contrast to the fixed-based simulator experiments, pilots did not assign Cooper-Harper ratings, due to the limited number of experimental runs.

Pilots received instructions for the different phases in flight. In accordance with the simulator task, pilots were instructed to fly at $\pm 1,000$ [*feet/min*] rate of climb during the test. However, the pilot was free to decide between ascent and descent, as long as the aircraft remains below FL135. This restriction was required, as a significant reduction of torque in the fly-by-wire system is activated above FL135. During the lateral handling tests, pilots were asked to assess differences between roll time constants. They decided on capturing a specific roll angle to investigate the performance of the system.

B. Results

1. Longitudinal response

The longitudinal tracking response of the controller can be seen in Figure 16, where the time on the horizontal axis represents the time passed after starting the controller in the aircraft. The pilot was requested to fly similar manoeuvres as in the simulator experiment. The controller was set with a CAP of 0.90 and a damping of 0.50 before 1,160 seconds. After 1,160 seconds the damping was changed to 0.15, whereas the CAP remained the same (indicated by the vertical black dotted line). The reference signal could not be followed properly at some time instants, since the elevator servo was saturated. This is indicated by the current in the actuator servo, I, which reaches the edges of the bandwidth (indicated by the horizontal black dotted lines). This is most visible at the 1,260 seconds

Downloaded by TU DELFT on January 6, 2020 | http://arc.aiaa.org | DOI: 10.2514/6.2020-0852

time point. In addition, some oscillations (which could be characterised as pilot-induced) were present for lower damping conditions. This is especially evident when comparing the pilot input to the reference signal between 1,270 and 1,300 seconds. The pilot also noticed this PIO himself when flying the aircraft. The lower damping was also identified by the pilot. The maximum $\Delta\delta_e$ during this run equalled $1.76 \cdot 10^{-3}$ [*rad*] or 1.01 [*deg*], whereas the maximum requested deflection by the controller equalled $3.91 \cdot 10^{-2}$ [*rad*] or 2.24 [*deg*].

The aircraft was properly trimmed before the run shown in Figure 16. The impact of improper trim is illustrated in Figure 17. Some manoeuvres were performed before the start of this run, which resulted in a mismatch between the trimmed and actual indicated airspeed of $\approx$ 10 [*m/s*]. The effect is seen in the actuator servo current *I*, where the initial value is not close to zero as indicated by the black line (in contrast to Figure 16). Additional actuator deflection was required to remain straight and steady flight at this higher speed, resulting in a nonzero current. The available bandwidth above the black line is smaller compared to the bandwidth below. This resulted in more actuator saturation and a lower maximum elevator deflection. Pilots indeed noticed this effect during flight, saying it was easier to control the aircraft in one direction compared to the other when the aircraft was not properly trimmed. A change of indicated airspeed of more than 5 [*m/s*] already resulted in this effect, according to the pilots. In addition, pilots noticed that the handling qualities of the aircraft were better when a lower pilot gain was used. This is confirmed in Figure 17, since higher stick deflections by the pilot result in more actuator saturation. The maximum $\Delta\delta_e$ during this run equalled $1.61 \cdot 10^{-3}$ [*rad*] or 0.917 [*deg*], whereas the maximum requested deflection by the controller equalled $1.43 \cdot 10^{-1}$ [*rad*] or 8.08 [*deg*].

2. Lateral response

The lateral tracking response of the aircraft during one of the runs is given in Figure 18. The fly-by-wire system shows similar limitations compared to the longitudinal response. The controller has proper tracking performance during the turn between 1,800 and 1,915 seconds. However, saturation also occurs in the aileron actuator servo if the pilot gives a larger input to the stick. This initially occurs at 1,940 seconds, but is more visible from 1,970 to 2,010 seconds. The servo current reaches the edges of the bandwidth which results in poor tracking performance. This poor tracking performance occasionally lead to pilot-induced oscillations in roll. The maximum $\Delta\delta_a$ during this run equalled $9.81 \cdot 10^{-2}$ [*rad*] or 5.62 [*deg*], whereas the maximum requested deflection by the controller equalled $2.59 \cdot 10^{-1}$ [*rad*] or 14.9 [*deg*].

C. Discussion and conclusions

Four flight tests were conducted to validate the variable stability controller. During the third and fourth flight test, the pilots noted that the response of the controller and the aircraft was similar to the experiment in the fixed-base simulator. This is confirmed by the comparison between the reference dynamics and the actual response of the aircraft. Due to time and cost limitations, the simulator experiment could not be exactly reproduced in the real flight test. However, pilots commented that they could notice differences between different damping settings, similar to the experiment in the

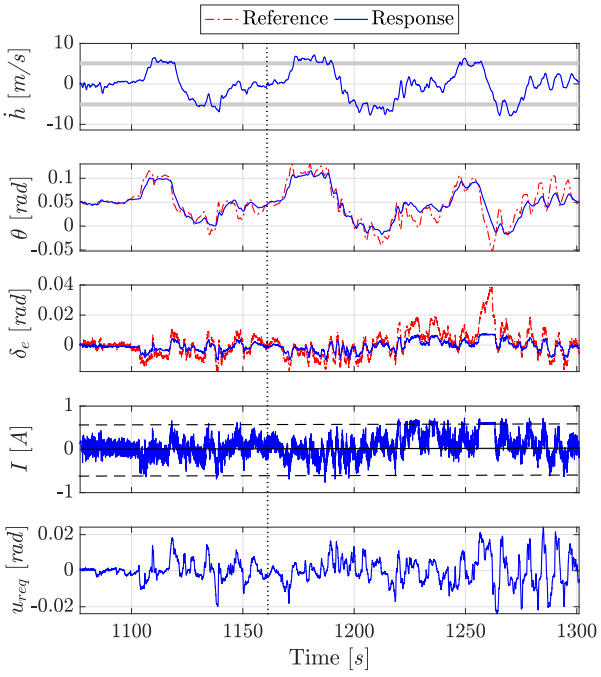

Fig. 16 Longitudinal tracking response (V_{ias} = 110 [*m/s*] FL130)

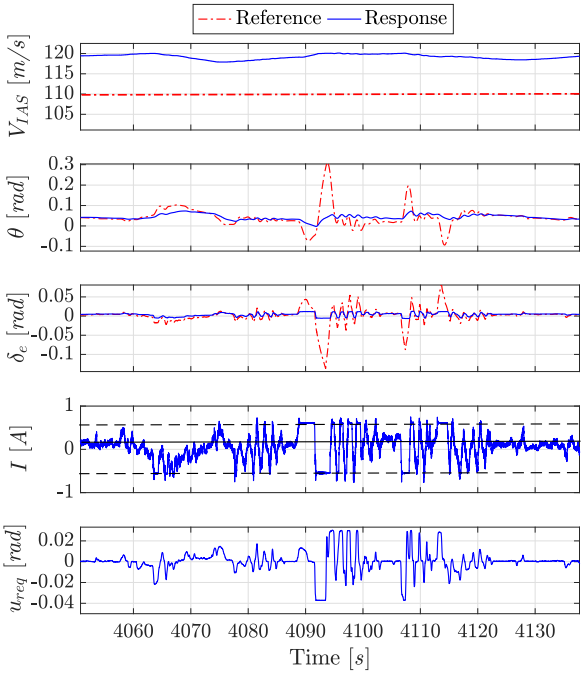

Fig. 17 Longitudinal tracking response (V_{ias} = 120 [*m/s*] FL130)

Downloaded by TU DELFT on January 6, 2020 | http://arc.aiaa.org | DOI: 10.2514/6.2020-0852

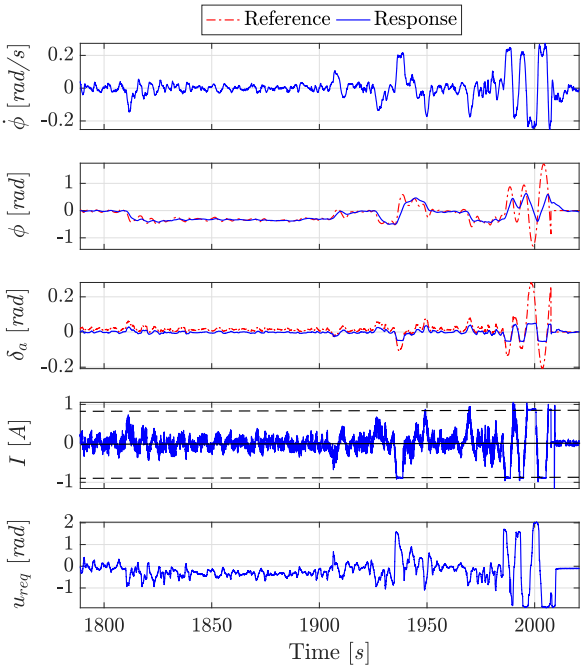

Fig. 18 Lateral tracking response (V_{ias} = 110 [*m/s*] FL130)

fixed-base simulator.

The system limitations were identified by pushing the system in roll and pitch whilst deviating from the initial trim condition. When the aircraft was within the performance bandwidth of the actuator servos, the INDI controller was able to track the reference signal quite well. It is expected that this can be further improved by implementing the aerodynamic model from the Cessna Citation II by Van den Hoek et al. [31], since the controller currently uses the aerodynamic model from the Citation I.

Actuator saturation is considered to be the most limiting factor, since tracking performance significantly decreases when saturation occurs. The requested deflection by the controller was in extreme cases both for the pitch as roll axis higher than the actual saturated deflection, by a factor of 8-10 in pitch and 3-4 in roll, respectively. This is by far the most limiting factor of the variable stability system performance.

The most obvious solution would be to replace the current fly-by-wire system with a more powerful system. This is however an expensive hardware change which requires re-certification. A possible improvement of the current system can be achieved by adding control of the elevator trim in the control laws. Future research should investigate whether a lower hinge moment can be achieved using the auto trim, without interfering with the actual response of the elevator. This could increase the performance band of the system in longitudinal motion but would also require hardware changes to the aircraft. Another solution would be to keep the auto trim activated and use the software model to predict when the auto trim is going to occur. This could then be used to minimise the interference of the auto trim on the actuator deflection. However, the expected non-linearities during flight limit the accuracy of any auto trim function predictions. This method is therefore considered a complicated alternative.

VII. Discussion and Recommendations

The purpose of this paper was twofold. First it was investigated whether an INDI controller can be used to create a variable stability in-flight simulator. Second, the limitations of the resulting system were researched. The controller was tested in offline simulations, during a fixed-base simulator experiment and in actual flight tests.

A. Handling qualities

The INDI technique is able to modify the handling qualities of an aircraft in a variable stability system. Offline simulations showed that the controller manipulates the response of the actuators to ensure tracking performance of the CAP reference model. The flight condition that provides the best performance for the Cessna Citation II laboratory aircraft was determined to be at 4, 000 [m] altitude with a true airspeed of 110 [*m/s*]. PCH improved the controller performance by slightly modifying the CAP reference signal when there was no actuator saturation present. However, the hedging signal adapted the CAP reference logic more significantly when the actuators were saturating. This implies that the handling qualities change when PCH is enabled, which is undesired behaviour.

An experiment was performed in a fixed-base simulator to determine whether pilots could notice the difference between the CAP reference model and a full model including the aircraft and actuator dynamics. The control activity of the pilots was higher for the full model compared to the CAP reference model, and the performance of the pilots was lower for the full model. These can both be explained by pilots who are not experiencing the expected response of the aircraft when actuators are saturating.

Pilots rated the full model on average two Cooper-Harper points lower compared to the reference dynamics model. It was hypothesised that this difference would occur due to actuator saturation. This was indeed confirmed by the differences of rating for the different CAP conditions. The CAP of 0.90 was rated at a mean Cooper-Harper difference of one, which differed statistically from the CAP of 0.45 and 0.25 with a mean Cooper-Harper difference of two. The CAP of 0.90 also showed a shorter maximum saturation time compared to the CAP of 0.25, whereas the difference between CAP 0.90 and 0.45 was close to the significance level. This confirmed the initial estimation of the system limitations. The actuator saturation data were compared with the Cooper-Harper differences between the CAP reference and the full model. The saturation time was used to update the model that estimates the handling quality limitations.

Flight tests were performed to validate the performance of the controller. Pilots noted that they experienced the changes in CAP and damping similar to the fixed-base simulator experiment. However, they also experienced some limitations to the system.

Downloaded by TU DELFT on January 6, 2020 | http://arc.aiaa.org | DOI: 10.2514/6.2020-0852

B. System limitations

Two factors were found to be limiting for the variable stability in-flight simulator using the INDI technique. The first factor was the accuracy of the moment effectiveness parameter. This parameter depends on the accuracy of both the aerodynamic coefficients and the aircraft inertia. During the offline simulations and the fixed-base experiment the controller showed proper tracking performance. Even in the flight tests, when additional non-linearities and disturbances are present, the INDI controller could track the reference model properly. This can be further improved, however, by updating the aerodynamic coefficients to the newer Cessna Citation II model.

The second and most limiting factor was found to be the actuator saturation. The tracking performance of the controller decreased significantly when actuator saturation occurred. Saturation occurred either when the input of the pilot was too high, or when the aircraft deviated too much from its initial trim condition. The maximum deflection of the elevator was approximately 1 [*deg*], whereas the maximum deflection of the ailerons was around 6 [*deg*]. These limited deflections arose from the constraints of the fly-by-wire system. Future research should investigate whether a lower hinge moment can be achieved using the auto trim, without interfering with the actual position of the elevator. This could increase the performance band of the system in longitudinal motion but would also require hardware changes to the aircraft.

VIII. Conclusions

This paper investigated whether the Cessna Citation II can be converted in a variable stability system, using incremental non-linear dynamic inversion. Offline simulations show that INDI can indeed be used to achieve a variable stability platform. Pseudo-Control Hedging increases the controller performance, but also affects the handling qualities. The simulator experiment showed that pilots could feel differences between the reference dynamics and a full model including actuators and the INDI controller. Pilots rate the full model on average two Cooper-Harper points lower compared to the reference dynamics model. The experienced model mismatch was higher for CAPs below the lower system limits as determined in the offline simulation, and actuator saturation increased for lower CAPs.

Four flight tests were conducted to validate the variable stability INDI controller in real flight. Pilots commented that they could notice differences between different damping settings, similar to the simulator experiment. System limitations were identified by pushing the system in roll and pitch whilst deviating from the initial trim condition. Especially the longitudinal motion was considered to be limited due to actuator saturation, which poses the main constraint on the developed system.

IX. Acknowledgements

The authors would like to thank the involved staff from the Delft University of Technology: Hans Mulder, Alexander in 't Veld, Menno Klaassen, Ferdinand Postema and Gijsbert den Toom. Their support, guidance and additional time during the project and especially the flight tests was highly appreciated. Finally, the authors would like to thank all pilots who participated in the experiments.

References

[1] Weingarten, N. C., "History of In-Flight Simulation at General Dynamics," *Journal of Aircraft*, Vol. 42, No. 2, 2005, pp. 290–298. doi:10.2514/1.4663.

[2] Hamel, P., *In-Flight Simulators and Fly-by-Wire / Light Demonstrators*, Springer Nature, 2017.

[3] Mirza, A., Van Paassen, M. M., and Mulder, M., "Simulator Evaluation of a Medium-Cost Variable Stability System for a Business Jet," *Proceedings of the AIAA Guidance, Navigation, and Control Conference*, 2019.

[4] Armstrong, E. S., *A Design System for Linear Multivariable Control*, New York: Marcel Dekker, 1980.

[5] O'Brien, M. J., and Broussard, J. R., ""Feedforward Control to Track the Output of a Forced Model." Decision and Control including the 17th Symposium on Adaptive Processes," *IEEE Conference on. IEEE*, 1979, pp. 835–842.

[6] Kreindler, E., and Rothschild, D., "Model-Following in Linear-Quadratic Optimization," *American Institute of Aeronautics and Astronautics Journal*, Vol. 14, no. 7, 1976, pp. 835–842.

[7] Slotine, J. J. E., and Li, W., *Applied Nonlinear Control*, Englewood Cliffs, N.J.: Prentice Hall, 1991.

[8] Ko, J., Lee, H., and Lee, J., "In Flight Simulation for Flight Control Law Evaluation of Fly-by-Wire Aircraft," *Agency for Defense Development, Daejeon, Republic of Korea*, 2004.

[9] Ko, J., and Park, S., "Variable stability system control law development for in-flight simulation of pitch/roll/yaw rate and normal load," *International Journal of Aeronautical and Space Sciences*, Vol. 15, No. 4, 2014, pp. 412–418. doi:10.5139/IJASS.2014.15.4.412.

[10] Miller, C., "Nonlinear Dynamic Inversion Baseline Control Law: Architecture and Performance Predictions," *AIAA Guidance, Navigation, and Control Conference*, Guidance, Navigation, and Control and Co-located Conferences, American Institute of Aeronautics and Astronautics, 2011. doi:10.2514/6.2011-6467, URL `https://doi.org/10.2514/6.2011-6467`.

[11] Smith, P., "A Simplified Approach to Non-linear Dynamic Inversion Based Flight Control," *23rd Atmospheric Flight Mechanics Conference*, 1998. doi:10.2514/6.1998-4461, URL `http://arc.aiaa.org/doi/10.2514/6.1998-4461`.

[12] Germann, K. P., *T-6A Texan II In-Flight Simulation and Variable Stability System Design*, Mississippi State University, 2006.

[13] Grondman, F., Looye, G., Kuchar, R. O., Chu, Q. P., and Van Kampen, E., "Design and Flight Testing of Incremental Nonlinear Dynamic Inversion-based Control Laws for a Passenger Aircraft," *2018 AIAA Guidance, Navigation, and Control Conference*, AIAA SciTech Forum, American Institute of Aeronautics and Astronautics, 2018. doi:10.2514/6.2018-0385, URL `https://doi.org/10.2514/6.2018-0385`.

Downloaded by TU DELFT on January 6, 2020 | http://arc.aiaa.org | DOI: 10.2514/6.2020-0852

[14] Lubbers, B., *A Model of the Experimental Fly-By-Wire Flight Control System for the PH-LAB*, Delft University of Technology (unpublished master thesis), 2009.

[15] Zaal, P., Pool, D. M., in 't Veld, A. C., Postema, F. N., Mulder, M., van Paassen, M. M., and Mulder, J. A., "Design and Certification of a Fly-by-Wire System with Minimal Impact on the Original Flight Controls," *AIAA Guidance, Navigation, and Control Conference*, 2009. doi:10.2514/6.2009-5985, URL http://arc.aiaa.org/doi/10.2514/6.2009-5985.

[16] Nelson, R. C., *Flight Stability and Automatic Control*, McGraw-Hill Education, 1998.

[17] Bryson, A. E., and Ho, Y. C., *Applied Optimal Control*, Hemisphere, Washington D.C., 1975.

[18] Ko, J., and Park, S., "Design of a Variable Stability Flight Control System," *KSAS International Journal*, Vol. 9, No. 1, 2008.

[19] Bacon, B., and Ostroff, A., "Reconfigurable Flight Control using Non-linear Dynamic Inversion with a special Accelerometer Implementation," *AIAA Guidance, Navigation, and Control Conference and Exhibit*, 2000. doi:10.2514/6.2000-4565, URL http://arc.aiaa.org/doi/10.2514/6.2000-4565.

[20] Cox, T., and Cotting, M., "A Generic Inner-Loop Control Law Structure for Six-Degree-of-Freedom Conceptual Aircraft Design," *43rd AIAA Aerospace Sciences Meeting and Exhibit*, Aerospace Sciences Meetings, American Institute of Aeronautics and Astronautics, 2005. doi:10.2514/6.2005-31, URL https://doi.org/10.2514/6.2005-31.

[21] Smeur, E. J. J., Chu, Q. P., and de Croon, G. C. H. E., "Adaptive Incremental Nonlinear Dynamic Inversion for Attitude Control of Micro Air Vehicles," *Journal of Guidance, Control, and Dynamics*, Vol. 39, No. 3, 2016, pp. 450–461. doi:10.2514/1.G001490.

[22] Smeur, E. J. J., de Croon, G. C. H. E., and Chu, Q. P., "Cascaded Incremental Nonlinear Dynamic Inversion Control for MAV Disturbance Rejection," *Control Engineering Practice*, Vol. 73, 2018, pp. 79–90.

[23] Cooper, G. E., and Harper, R. P., "Handling Qualities and Pilot Evaluation," *Journal of Guidance, Control, and Dynamics*, Vol. 9, No. 5, 1986, pp. 515–529. doi:10.2514/3.20142.

[24] Bihrle, W., "A Handling Qualities Theory for Precise Flight Path Control," Tech. rep., Air Force Flight Dynamics Laboratory, New York, 1966.

[25] Standard, *MIL-STD-1797A Requirements for Flying Qualities of Piloted Aircraft*, Department of Defense, 1990.

[26] Bischoff, D. E., "The Control Anticipation Parameter for Augmented Aircraft," Tech. rep., Naval Air Development Center, Warminster, 1981.

[27] Di Franco, D. A., "In-flight Investigation of the Effects of Higher-Order Control System Dynamics on Longitudinal Handling Qualities," Tech. rep., Cornel Aeronautic Lab, Buffalo NY, 1968. doi:10.1002/nav.3800080206.

[28] Hodgkinson, J., LaManna, W. J., and Heyde, J. L., "Handling Qualities of Aircraft with Stability and Control Augmentation Systems - A Fundamental Approach," Vol. 80, 1976, pp. 75–81.

[29] Morelli, E. A., *Identification of Low Order System Models From Flight Equivalent Test Data*, NASA Langley Research Center, 2000.

[30] Borst, C., *CITAST: Citation Analysis and Simulation Toolkit*, Delft University of Technology, Delft, 2004.

[31] Van den Hoek, M. A., de Visser, C. C., and Pool, D. M., "Identification of a Cessna Citation II Model Based on Flight Test Data," *Advances in Aerospace Guidance, Navigation and Control*, 2018, pp. 259–277.

[32] Johnson, E. N., and Calise, A. J., "Pseudo-Control Hedging : a New Method for Adaptive Control," *Advances in Navigation Guidance and Control Technology Workshop*, 2000.

[33] Looye, G., Thümmel, M., Kurze, M., Otter, M., and Bals, J., "Non-linear Inverse Models for Control," *Proceedings of the 4th Modelica Conference*, 2005, pp. 267–279.

[34] van Paassen, M. M., Stroosma, O., and Delatour, J., "DUECA - Data-driven Activation in Distributed Real-Time Computation," *Modeling and Simulation Technologies Conference*, Guidance, Navigation, and Control and Co-located Conferences, American Institute of Aeronautics and Astronautics, 2000. doi:10.2514/6.2000-4503, URL https://doi.org/10.2514/6.2000-4503.

Downloaded by TU DELFT on January 6, 2020 | http://arc.aiaa.org | DOI: 10.2514/6.2020-0852